Thermal Conductivity Enhancement of Metal-organic Frameworks Employing Mixed Valence Metal Doping Technique

Jahan, Israt
Mechanical Engineering Department, Kyushu University

Bidyut Baran Saha
Mechanical Engineering Department, Kyushu University

https://doi.org/10.5109/4102458

出版情報：Proceedings of International Exchange and Innovation Conference on Engineering & Sciences (IEICES). 6, pp.20-26, 2020-10-22. 九州大学大学院総合理工学府
バージョン：
権利関係：

Thermal Conductivity Enhancement of Metal-organic Frameworks Employing Mixed Valence Metal Doping Technique

Israt Jahan[1], Bidyut Baran Saha[1,2]
[1] Mechanical Engineering Department, Kyushu University, 744 Motooka, Nishi-ku, Fukuoka 819-0395, Japan
[2] International Institute for Carbon-Neutral Energy Research (WPI-I2CNER), Kyushu University, 744 Motooka, Nishi-ku, Fukuoka 819-0395, Japan
Corresponding author email: saha.baran.bidyut.213@m.kyushu-u.ac.jp

ABSTRACT: *Excellent adsorption properties of porous metal-organic frameworks (MOFs) render them highly potential adsorbent for adsorption heat pump applications. However, their thermal properties are not quite satisfactory. Aluminium fumarate is a bioavailable ligand-based metal-organic framework with promising water uptake capacity. In this study, aluminium fumarate was synthesized following a green synthesis route and was doped with Nickel and Cobalt material at 10% and 20% concentration to create a mixed-valence complex system. Their thermal diffusivity and thermal conductivity were studied at different compression (7 MPa, 17 MPa and 27 MPa) pressure over a temperature range of 30 °C to 110 °C. Metal doping enhances the thermal conductivity of the doped aluminium fumarate MOFs. Doping of cobalt has a greater effect compared to nickel and 20% cobalt doped aluminium fumarate shows the highest thermal conductivity at 7 MPa compression pressure.*

Keywords: Metal-organic Frameworks; Metal Doping; Thermal Conductivity, Packing Density.

1. INTRODUCTION

A major portion of global energy consumption is liable for providing heating or cooling towards households as well as to industries. Large energy production accounts for environmental pollutions by particulate emission, fuel burning and so many negative impacts. Hence, an alternative technology to provide cooling without consumption of large amount of electricity is obligatory. Such an energy efficient alternative technology is adsorption heat pump which is driven by low grade thermal energy. The major strength of adsorption driven heat pump is that it is operated by low driving temperature (below 100 °C) for regeneration of adsorbents, which could be supplied by industrial waste heat or solar energy [1]. Industrial waste heat could be supplied from flue gases from boiler, waste gas from furnace, kiln, oven, exhaust from dryers and so on [2]. Moreover, it employs non-toxic working fluids (water, ethanol, carbon di-oxide) as refrigerants.

The technology of adsorption heat pump was invented a long ago. The cooling effect of silver chloride – ammonia pair was first observed by Micheal Faraday in 1823 and first commercial application of adsorptive based cooling system was by US railways using silica gel – Sulphur dioxide working pair in 1929 [3]. However, the vapor compression based cooling technology swiftly put back adsorption based technology due to its high efficiency and availability of CFC refrigerants. Adsorption cooling system came again in focus of attention of the researchers in the 80's when concern raised against the use of CFCs due to its ozone layer depletion and greenhouse effect which eventually results in imposition of "Montreal protocol" (1979) and "Kyoto protocol" (1987) [4].

Afterwards many researchers are studying on adsorption cooling system to enhance the system performance applying different adsorbents and adsorbent-adsorbate working pairs. The most studied adsorbents are silica gels [5][6], zeolites [7][8] and Carbon based compounds [9–13] with water, ethanol and carbon di-oxide as working fluids. Nowadays, metal-organic frameworks are drawing attentions as favorable adsorbent due to their high porous properties and great affinity towards water.

Metal-organic frameworks (MOFs) are a class of organometallic crystalline compounds composed of inorganic metals and organic ligands. Inorganic metal clusters are linked by polydentate organic ligands and create highly porous crystalline structure. The metal ion coordinated with bonding atoms (generally oxygen or nitrogen) of ligands are termed as metal nodes [14]. Diversity of organic ligands and metal nodes offers the opportunity to design a large number of MOFs. Multitudinous MOFs can be constructed with varying properties in its structure, porosity, topology and surface area. Physiochemical properties of metal-organic frameworks can be functionalized for different specific applications. Such promising features as tunable structure, highly compatible pore size, impressive porosity and unprecedentedly high surface area render MOFs towards diverse potential applications. Owing to be highly porous materials, metal-organic frameworks are limited to application due to their low thermal conductivity. This low thermal property of MOFs is caused by their short mean phonon path and low atomic density.

Thermal conductivity of adsorbents is a crucial property for the overall performance of the system. Thermal conductivity is an intrinsic property of a material which describes its heat conduction ability. It is defined as the amount of heat transferred by a material per unit time, per unit area to increase its temperature by one unit. If the adsorbent possess low thermal conductivity, heat transfer through the adsorbent bed will be slower. This will hinder adsorbent reach the desired adsorption or desorption temperature and consequently the total period of adsorption and desorption period will be lengthy rendering the system less efficient. Hence, increasing

thermal properties of adsorbents are intriguing research avenues. Many researchers studied different ways of increasing thermal properties of adsorbent materials. Animesh et. al.[15] prepared composites of material having high adsorption capacity with high conductive material to enhance the thermal conductivity of the sample.

In situ doping of metal ions in MOFs may also have positive effect on thermal properties. In our previous studies, we investigated the adsorption capacity of aluminum fumarate and nickel and cobalt doped aluminium fumarate [16,17] and thermophysical properties of this materials at room temperature [18].

In this present study, we studied the experimental measurement of thermal conductivity of hydrothermally synthesized aluminum fumarate for a wide range of temperature and three different compression pressures. The pristine aluminium fumarate MOF was modified by in situ doping of two transition metals nickel and cobalt at different concentrations. The effect of compression pressure and metal doping in thermal properties of aluminum fumarate was studied. Doping of different transition metals significantly affect the thermal properties of the pristine MOF.

2. EXPERIMENTAL

2.1 Materials

The chemicals used for the synthesis of the MOF samples are aluminium sulphate octadecahydrate [$Al_2(SO_4)_3.18H_2O$), 666.4 g/mol] and fumaric acid [$C_4H_4O_4$, 116.07 g/mol] from Waco Pure Chemical Industries; nickel chloride [$NiCl_2$, 129.6 g/mol], cobalt chloride [$CoCl_2$], and sodium hydroxide [NaOH, 40 g/mol] from Sigma Alddrich Co. Pure distilled water was used as solvent. All the chemicals were used without further purification.

2.2 Synthesis of samples

2.2.1 Aluminium fumarate

Aluminium fumarate was synthesized according to previously published procedure[16]. We followed the hydrothermal synthesis procedure to exclude the use of toxic and hazardous organic solvents like DMF (N, N-dimethylformamide). The synthesis procedure is presented in Fig. 1

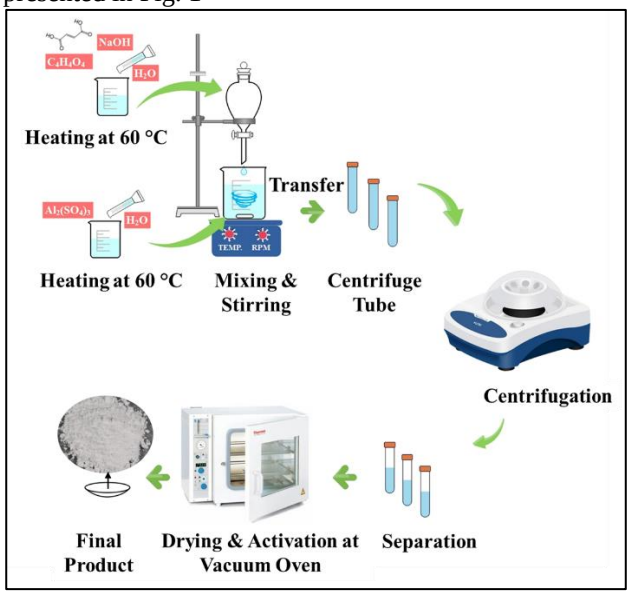

Fig. 1. Synthesis steps of aluminium fumarate MOF

Briefly, 1 eq. of aluminum sulphate was dissolved in distilled water. In another beaker 2 eq. of fumaric acid was dissolved in water by addition of 6 eq. of sodium hydroxide. Fumaric acid get dissolved in water by base diffusion technique. Both the solutions were heated up to 60 °C temperature and the former solution was added to the later dropwise with stirring in an electric heater equipped with magnetic stirrer. White milky solution was formed. The mixture was allowed to cool down to room temperature and separated using a centrifuging machine. The product was washed with water thrice to remove the chloride ion and any unreacted reagents remaining. The final product was dried overnight at 80 °C and activated at 120 °C in a vacuum oven.

2.2.2 10% and 20% Ni doped aluminium fumarate

10% and 20% Ni doped aluminium fumarate was prepared following the similar process as described above. A mixture of 90 wt% of aluminium salt and 10 wt% of nickel salt and 80 wt% of aluminium salt and 20 wt% of nickel salt and was used to prepare the salt solution. The linker solution and the further procedure was same as that of aluminium fumarate.

2.2.3 10% and 20% Co doped aluminium fumarate

10% and 20% Co doped aluminium fumarate MOFs was prepared in the similar synthesis procedure of Ni doped aluminium fumarate MOFs.

2.3 Thermal Conductivity

Thermal conductivity of the samples was computed from thermal diffusivity, packing density and specific heat capacity values of the samples from equation 12

The thermal diffusivity of the samples was determined by using LFA 457 MicroFlash Laser Flash Instrument from NETZSCH. A schematic diagram of the instrument is shown in **Fig. 2**. The major components of the system are the furnace, laser source, infrared radiation (IR) detector unit and the data acquisition system. LFA 457 MicroFlash measure thermal diffusivity according to the highly acknowledged Flash method.

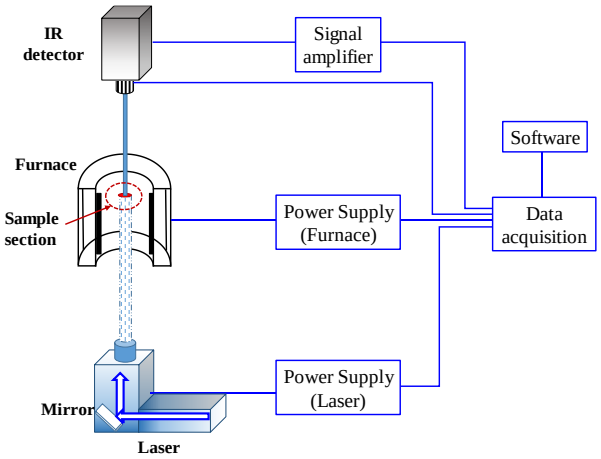

Fig. 2. Schematic presentation of LFA 457 system.

A short laser pulse from the laser source is guided by a mirror to the sample placed in a sample holder in the furnace and heat up the sample in its front side. The heat

that get adsorbed, propagates through the sample and heat up the rear surface of the sample. The IR detector set at the top of the machine, directing to the furnace, measure the resulting temperature rise in the rear surface as a function of time. From the detector signal the half time, $t_{0.5}$ (time required to reach the half height of the signal) is calculated and this half time and sample thickness is used to calculate the thermal diffusivity (eq. 2).

This laser flash method was first introduced by Parker et al. [19] by considering a one-dimensional heat conduction in a thermally insulated solid of uniform thickness l. Let the initial temperature distribution be T(x,0). The temperature distribution within the solid T(x,t) satisfies the 1-D heat conduction equation [20].

$$\frac{\partial T}{\partial t} = a\frac{\partial^2 T}{\partial t^2} \qquad (1)$$

Here, T(x,t) denotes the temperature of the sample at any time t and position x. Carslaw and Jaeger [21] derived a solution to the equation as

$$a = 1.3888\frac{l^2}{t_{0.5}} \qquad (2)$$

Using this equation (2), thermal diffusivity (a) is determined from the sample thickness (l) and half time ($t_{0.5}$).

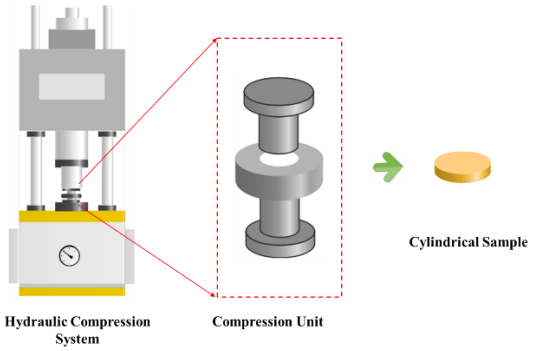

Fig. 3. Schematic presentation of hydraulic compression system

To prepare disk shaped samples for thermal diffusivity measurement, the MOF samples were compacted in a hydraulic compression system. Aluminium fumarate and metal doped aluminium fumarate MOF samples consolidated without use of any binder. To investigate the effect of compression pressure on the thermal properties of MOF samples three different compression pressure was used. Each samples were consolidated at 7 MPa, 17 MPa and 27 MPa pressure.

Thickness of the sample was measured by QuantuMike micrometer. The packing density (ρ, gcm^{-3}) was calculated from the thickness and mass.

From the calculated packing density and thermal diffusivity data from LFA, the thermal conductivity, K [unit, $Wm^{-1}\ K^{-1}$] was finally calculated by using the equation (3),

$$K = a \times C_p \times \rho \qquad (3)$$

3. RESULT AND DISCUSSION

Thermal diffusivity of aluminium fumarate, 10% Ni-aluminium fumarate (10% Ni-ALF), 20% Ni-aluminium fumarate (20% Ni-ALF), 10% Co-aluminium fumarate (10% Co-ALF) and 20% Co-aluminium fumarate (20% Co-ALF) MOF samples were measured over a wide range of temperature, from 30°C to 110 °C. All the samples were compressed at 7 MPa, 17 MPa and 27 MPa pressure during sample preparation steps. At every single temperature five shots were taken to confirm reproducibility of results. The results show negligible variance in results at each temperature. Specific heat capacity data, C_p of each sample was taken our previously reported work [18]. The data was calculated from the equation of Green and Perry model [22] using the value of adjustable parameters, α, β and γ published by Jahan et. al. [18].

$$C_p = \alpha + \beta T + \frac{\gamma}{T^2} \qquad (9)$$

The specific heat capacity data of the samples are presented in table 1. Packing density, ρ of the samples were calculated from mass and sample thickness of the samples. From the packing density, specific heat capacity data and thermal diffusivity, the thermal conductivity of the samples was calculated. The thermal properties of the samples are discussed below.

Table 1. Specific heat capacity values of the samples

Temperature, (°C)	Specific heat capacity, (kJ $kg^{-1}\ K^{-1}$)				
	Aluminium fumarate	10% Ni-aluminium fumarate	20% Ni-aluminium fumarate	10% Co-aluminium fumarate	20% Co-aluminium fumarate
30	1.330	1.256	1.234	1.274	1.178
40	1.323	1.257	1.235	1.284	1.182
50	1.332	1.261	1.239	1.298	1.193
60	1.339	1.268	1.244	1.315	1.206
70	1.347	1.276	1.250	1.333	1.220
80	1.356	1.284	1.256	1.351	1.235
90	1.366	1.294	1.263	1.370	1.250
100	1.375	1.303	1.270	1.388	1.266
110	1.448	1.397	1.340	1.407	1.281

Aluminium Fumarate:

The thermal conductivity values of aluminium fumarate samples prepared at 7 MPa, 17 MPa and 27 MPa are shown in figure 3 and the packing density of these samples are shown in Fig. *5*. Thermal conductivity values show an increase with increasing temperature and packing density increases with increasing compression pressure. At high compression pressure the samples get more compacted and raise the packing density. As the compression pressure increases the thermal conductivity value also increases. This increase in thermal conductivity can be contributed to the high packing density. In highly compacted samples, particles remain closely contacted which facilitate the transfer of heat and results in high thermal conductivity. The increased thermal conductivity value with compression pressure also indicate the retention of structural integrity even in high consolidation pressure.

Nickel-doped Aluminium Fumarate

A comparison of Nickel- doped samples with pristine aluminium fumarate sample at 7 MPa, 17 MPa and 27 MPa are shown in Fig. 6,

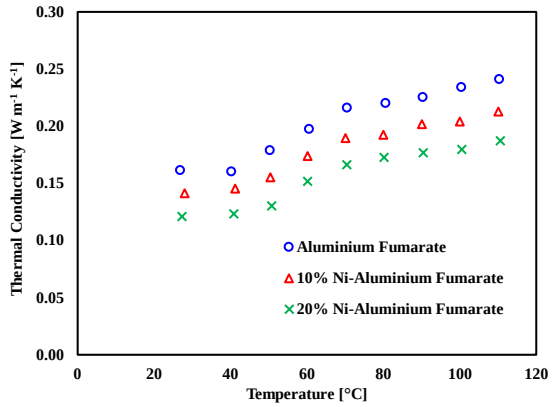

Fig. 7 and Fig. 8 respectively. Both samples show an increase in thermal conductivity with increasing temperature. At 7 MPa 10% Ni-ALF shows a slight increase in thermal conductivity over pristine aluminium fumarate. 20% Ni-ALF shows slight increase in thermal conductivity in lower temperature range but decreases at higher temperature (over 60 °C). These results indicate that transient metal doping significantly affect the thermal properties of the MOF samples. Chloride salt of Nickel contains divalent nickel ion (Ni^{2+}), which when substituted in the aluminium fumarate metal organic framework, create a mixed valance system since aluminium gives a trivalent ion (Al^{3+}). In a mixed valance system charge mobility increases due to formation of electron delocalization [23]. This increase charge mobility and high packing density may contribute to the increased thermal conductivity of the samples.

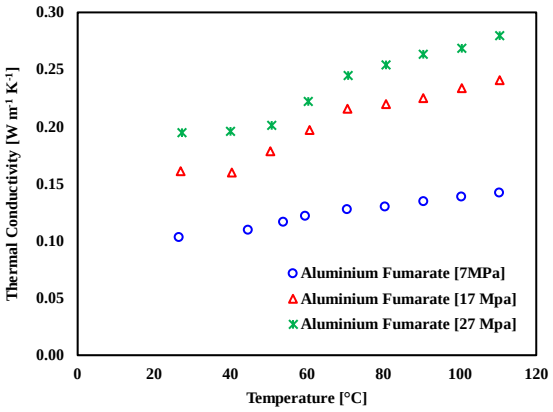

Fig. 4. Plot of thermal conductivity aluminium fumarate at different compression pressure

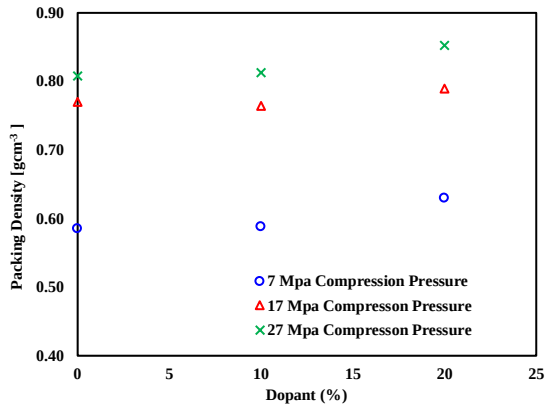

Fig. 5. Packing density of Nickle doped aluminium fumarate

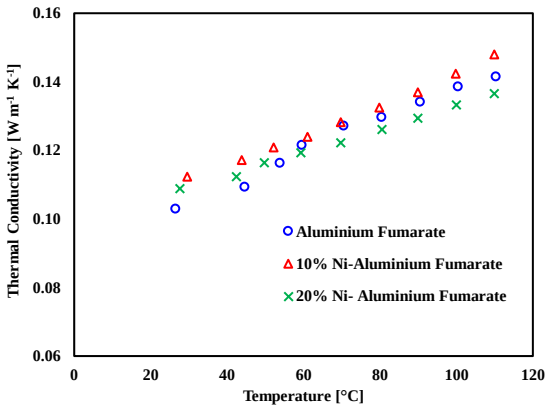

Fig. 6. Comparison of thermal conductivity of 10% and 20% nickel doped aluminium fumarate with parent aluminium fumarate at 7 MPa compression pressure

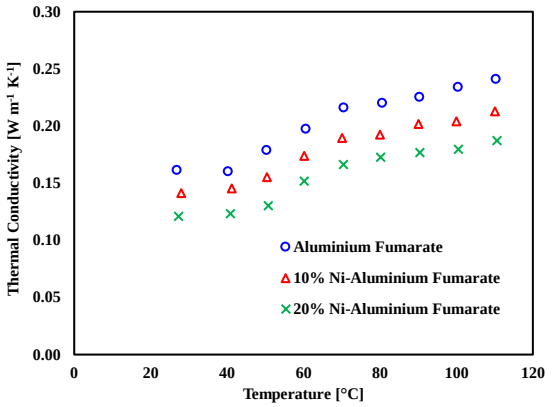

Fig. 7 and Fig. 8 presents the comparison of thermal conductivity of samples of aluminium fumarate, 10% Ni-aluminium fumarate and 20% Ni-aluminium fumarate prepared at 17 MPa and 27 MPa compression pressure respectively. From the results it is shown that though packing density increases with increasing compression pressure (Fig. 5), their thermal conductivity does not increase as well. Higher compression pressure may cause structural distortion in Nickel doped MOFs [24] and affect their performance.

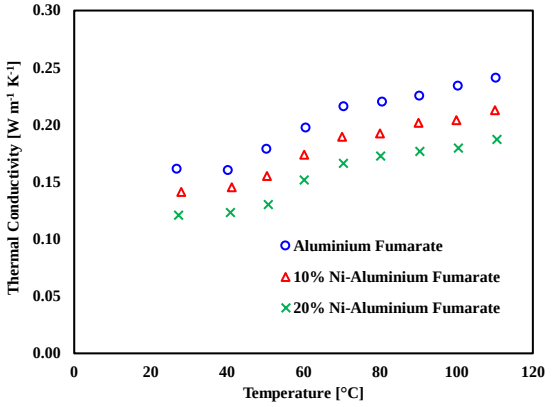

Fig. 7. Comparison of thermal conductivity of 10% and 20% nickel doped aluminium fumarate with parent aluminium fumarate at 17 MPa compression pressure

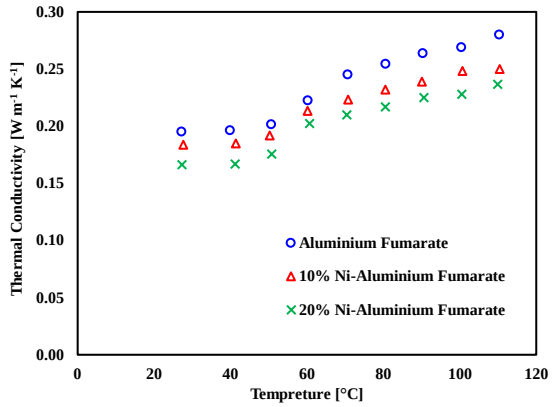

Fig. 8. Comparison of thermal conductivity of 10% and 20% nickel doped aluminium fumarate with parent aluminium fumarate at 27 MPa compression pressure

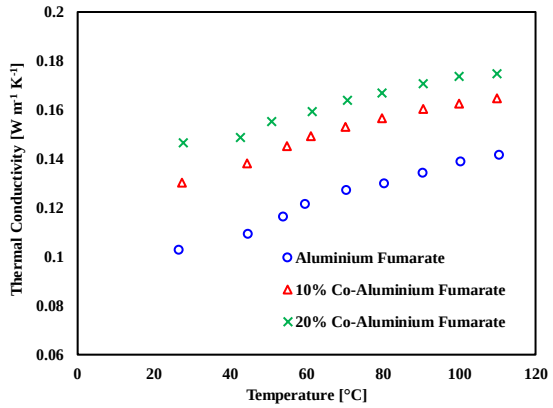

Fig. 9. Comparison of thermal conductivity of 10% and 20% cobalt doped aluminium fumarate with parent aluminium fumarate aluminium fumarate at 7 MPa compression pressure.

Cobalt-doped Aluminium Fumarate

The comparison of 10% and 20% Co-aluminium fumarate with parent MOF of samples prepared at & MPa compression pressure is presented in Fig. 9. And packing density of cobalt doped MOFs at different compression pressure is shown in Fig. 10. Thermal conductivity of cobalt doped MOFs show a sharp increase in their value compared to the parent MOF and thermal conductivity of the samples increase with temperature. This increased thermal property can be attributed to the high packing density of the samples with incorporation of dopants and to the increased charged mobility of a mixed valence system. When Co^{2+} ion is incorporated in the crystal system of aluminium (Al^{3+}) fumarate, it may cause charge delocalization as well as increased charge mobility. Both the effects improve the final thermal conductivity of the Co- doped samples.

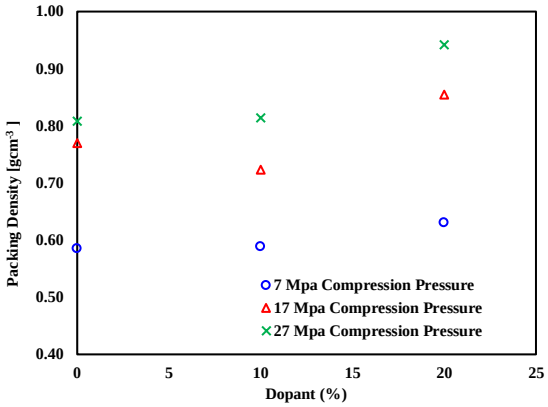

Fig. 10. Packing density of Cobalt doped aluminium fumarate

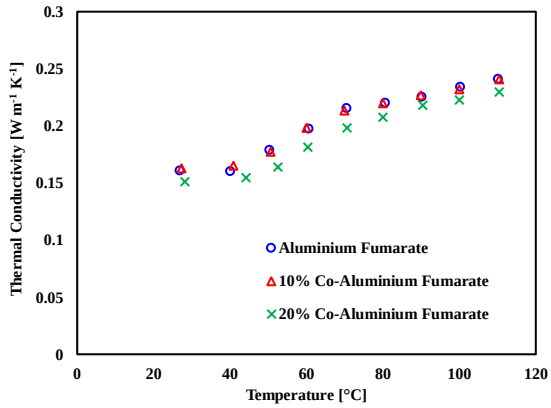

Fig. 11. Comparison of thermal conductivity of 10% and 20% cobalt doped aluminium fumarate with parent aluminium fumarate at 17MPa compression pressure

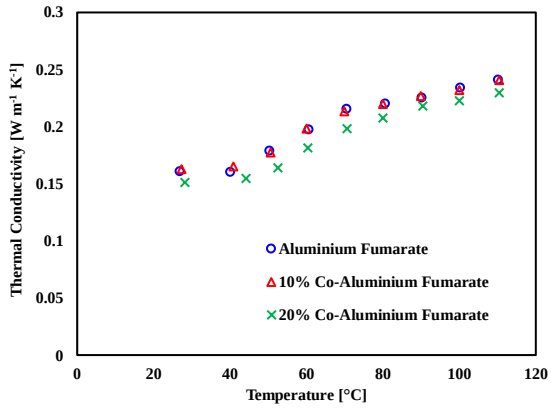

Fig. 11 and Fig.12 show the comparison of the thermal conductivity of cobalt doped samples with aluminium fumarate at 17 MPa and 27 MPa respectively. From Fig. 10 it is found that packing density of the cobalt doped samples increase with increasing compression pressure. However, as like nickel doped aluminium fumarates, Cobalt dopes MOFs also showed poor performance at higher compression pressure. Cobalt doped MOFs also cannot retain their structural integrity. Since doping of a divalent metal ion in a trivalent MOF system create a complex structure, it may cause structural collapse at higher pressure and their performance downgrade.

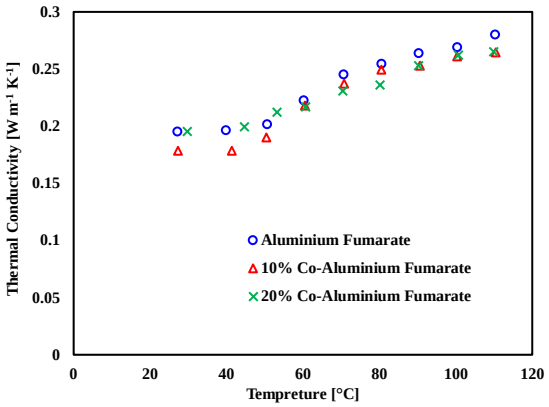

Fig.12. Comparison of thermal conductivity of 10% and 20% cobalt doped aluminium fumarate with parent aluminium fumarate at 27MPa compression pressure

4. CONCLUSION

In this study, aluminium fumarate, 10% and 20 % nickel doped aluminium fumarate and 10% and 20% cobalt doped aluminium fumarate was synthesized following a green synthesis process. Subsequently, thermal properties of the parent and doped MOF samples were determined over a long range of temperature starting from 30 °C to 110 °C. To evaluate the retention of the performance of the samples upon high compression pressure the samples were prepared at 7 MPa, 17 MPa and 27 MPa and investigated for thermal properties. Doping of transition metals at 7 MPa pressure increase the thermal conductivity compared to the parent MOF. Cobalt doping enhance the thermal properties greatly compared to Nickel doping. 20 % Co-aluminium fumarate showed the highest thermal conductivity. However, at higher compression pressure (17 MPa and 27 MPa) the doped MOFs loss their performance. Hereinafter, it can be said that mixed valence metal doping is an efficient way to increase thermal properties of porous MOF structures as well as to improve their performance in the adsorption cooling system.

REFERENCES

[1] B.B. Saha, K. Uddin, A. Pal, K. Thu, Emerging sorption pairs for heat pump applications: an overview, JMST Adv. 1 (2019) 161–180. https://doi.org/10.1007/s42791-019-0010-4.

[2] J. Ling-Chin, State-of-the-Art Technologies on Low-Grade Heat Recovery and Utilization in Industry, in: H. Bao (Ed.), IntechOpen, Rijeka, 2019: p. Ch. 4. https://doi.org/10.5772/intechopen.78701.

[3] M.F. de Lange, K.J.F.M. Verouden, T.J.H. Vlugt, J. Gascon, F. Kapteijn, Adsorption-Driven Heat Pumps: The Potential of Metal–Organic Frameworks, Chem. Rev. 115 (2015) 12205–12250. https://doi.org/10.1021/acs.chemrev.5b00059.

[4] H. Demir, M. Mobedi, S. Ülkü, A review on adsorption heat pump: Problems and solutions, Renew. Sustain. Energy Rev. 12 (2008) 2381–2403. https://doi.org/https://doi.org/10.1016/j.rser.2007.06.005.

[5] K.C. Ng, H.T. Chua, C.Y. Chung, C.H. Loke, T. Kashiwagi, A. Akisawa, B.B. Saha, Experimental investigation of the silica gel–water adsorption isotherm characteristics, Appl. Therm. Eng. 21 (2001) 1631–1642. https://doi.org/https://doi.org/10.1016/S1359-4311(01)00039-4.

[6] A. Khalil, E.-S.A. El-Agouz, Y.A.F. El-Samadony, M.A. Sharaf, Experimental study of silica gel/water adsorption cooling system using a modified adsorption bed, Sci. Technol. Built Environ. 22 (2016) 41–49. https://doi.org/10.1080/23744731.2015.1072454.

[7] T. Miltkau, B. Dawoud, Dynamic modeling of the combined heat and mass transfer during the adsorption/desorption of water vapor into/from a zeolite layer of an adsorption heat pump, Int. J. Therm. Sci. 41 (2002) 753–762. https://doi.org/https://doi.org/10.1016/S1290-0729(02)01369-8.

[8] S. Kayal, S. Baichuan, B.B. Saha, Adsorption characteristics of AQSOA zeolites and water for adsorption chillers, Int. J. Heat Mass Transf. 92 (2016) 1120–1127. https://doi.org/https://doi.org/10.1016/j.ijheatmasstransfer.2015.09.060.

[9] A. Pal, K. Uddin, K. Thu, B.B. Saha, Activated carbon and graphene nanoplatelets based novel composite for performance enhancement of adsorption cooling cycle, Energy Convers. Manag. 180 (2019) 134–148. https://doi.org/10.1016/J.ENCONMAN.2018.10.092.

[10] K. Uddin, M.A. Islam, S. Mitra, J. Lee, K. Thu, B.B. Saha, S. Koyama, Specific heat capacities of carbon-based adsorbents for adsorption heat pump application, Appl. Therm. Eng. 129 (2018) 117–126. https://doi.org/10.1016/j.applthermaleng.2017.09.057.

[11] A. Pal, K. Uddin, K.A. Rocky, K. Thu, B.B. Saha, CO2 adsorption onto activated carbon–graphene composite for cooling applications, Int. J. Refrig. 106 (2019) 558–569. https://doi.org/https://doi.org/10.1016/j.ijrefrig.2019.04.022.

[12] T. Kawano, M. Kubota, M.S. Onyango, F. Watanabe, H. Matsuda, Preparation of activated carbon from petroleum coke by KOH chemical activation for adsorption heat pump, Appl. Therm. Eng. 28 (2008) 865–871. https://doi.org/https://doi.org/10.1016/j.applthermaleng.2007.07.009.

[13] K.A. Rocky, A. Pal, B.B. Saha, Adsorption Characteristics of CO2 onto Carbon Nanotube for Adsorption Cooling / Capturing Applications, Proceeding Int. Exch. Innov. Conf. Eng. Sci. (2019) 67–69. https://doi.org/https://doi.org/10.15017/2552939.

[14] H. Furukawa, K.E. Cordova, M. O'Keeffe, O.M. Yaghi, The Chemistry and Applications of Metal-Organic Frameworks, Science (80-.). 341 (2013).

[15] A. Pal, K. Uddin, K. Thu, B.B. Saha, Activated carbon and graphene nanoplatelets based novel composite for performance enhancement of adsorption cooling cycle, Energy Convers. Manag. 180 (2019) 134–148. https://doi.org/10.1016/j.enconman.2018.10.092.

[16] M.L. Palash, I. Jahan, T.H. Rupam, S. Harish, B.B. Saha, Novel technique for improving the water adsorption isotherms of metal-organic frameworks for performance enhancement of adsorption driven chillers, Inorganica Chim. Acta. 501 (2020) 119313. https://doi.org/10.1016/J.ICA.2019.119313.

[17] T. Hasan, Adsorption Characterization of Aluminum Fumarate Metal-organic Framework, (2019) 34–35.

[18] I. Jahan, M.A. Islam, M.L. Palash, K.A. Rocky, T.H. Rupam, B.B. Saha, Experimental Study on the Influence of Metal Doping on Thermophysical Properties of Porous Aluminum Fumarate, Heat Transf. Eng. (2020) 1–10. https://doi.org/10.1080/01457632.2020.1777005.

[19] W.J. Parker, R.J. Jenkins, C.P. Butler, G.L. Abbott, Flash method of determining thermal diffusivity, heat capacity, and thermal conductivity, J. Appl. Phys. 32 (1961) 1679–1684. https://doi.org/10.1063/1.1728417.

[20] M. Yoneda, S. Kawabata, Analysis of Transient Heat Conduction and its Applications, J. Text. Mach. Soc. Japan. 29 (1983) 73–83. https://doi.org/10.4188/jte1955.29.73.

[21] H.S. (Horatio S. Carslaw, 1907-1979 Jaeger J. C. (John Conrad), Conduction of heat in solids, 2nd ed, Oxford : Clarendon Press, 1959.

[22] D.W. Green, R.H. Perry, J.O. Maloney, Perry's chemical engineer's handbook, 7th ed., McGraw-Hill Publishing Company, New York, NY, 1997.

[23] J.G. Park, M.L. Aubrey, J. Oktawiec, K. Chakarawet, L.E. Darago, F. Grandjean, G.J. Long, J.R. Long, Charge Delocalization and Bulk Electronic Conductivity in the Mixed-Valence Metal–Organic Framework Fe(1,2,3-triazolate)2(BF4)x, J. Am. Chem. Soc. 140 (2018) 8526–8534. https://doi.org/10.1021/jacs.8b03696.

[24] M. Taddei, M.J. McPherson, A. Gougsa, J. Lam, J. Sewell, E. Andreoli, An optimised compaction process for zr-fumarate (MOF-801), Inorganics. 7 (2019). https://doi.org/10.3390/inorganics7090110.